Capturing the Transition From Intermediate to Neovascular AMD: Longitudinal Inner Retinal Thinning and Factors Associated With Neuronal Loss

Enrico Borrelli,[1,2] Costanza Barresi,[1,2] Giorgio Lari,[1,2] Alessandro Berni,[1,2] Marco Battista,[1,2] Michele Reibaldi,[3] Maria Lucia Cascavilla,[1,2] and Francesco Bandello[1,2]

[1]Vita-Salute San Raffaele University, Milan, Italy
[2]IRCCS San Raffaele Scientific Institute, Milan, Italy
[3]Department of Ophthalmology, University of Turin, Turin, Italy

Correspondence: Enrico Borrelli, Department of Ophthalmology, Vita-Salute San Raffaele University, Via Olgettina 60, Milan, Italy; borrelli.enrico@yahoo.com.

EB and CB contributed equally to the work presented here and should therefore be regarded as equivalent authors.

Received: August 19, 2022
Accepted: April 2, 2023
Published: April 19, 2023

Citation: Borrelli E, Barresi C, Lari G, et al. Capturing the transition from intermediate to neovascular AMD: Longitudinal inner retinal thinning and factors associated with neuronal loss. *Invest Ophthalmol Vis Sci.* 2023;64(4):21. https://doi.org/10.1167/iovs.64.4.21

Purpose. To estimate the impact of transition from intermediate to exudative neovascular age-related macular degeneration (AMD) on the inner retina and to assess the relationship of clinical characteristics and optical coherence tomography (OCT) findings with inner retinal changes.

Methods. A total of 80 participants (80 eyes) with intermediate AMD at baseline who developed neovascular AMD within 3 months were included in the analysis. OCT scans at follow-up visits (after transition to neovascular AMD) were compared with values at the latest visit with evidence of intermediate AMD to quantify longitudinal inner retinal changes. OCT images were also reviewed for qualitative features reflecting distress of the outer retina or retinal pigment epithelium and for the presence and characteristics of exudation.

Results. The parafoveal and perifoveal inner retinal thicknesses were 97.6 ± 12.9 µm and 103.5 ± 16.2 µm, respectively, at baseline, and a significant increase in values was detected at the visit with first evidence of neovascular AMD (parafoveal: 99.0 ± 12.8 µm, $P = 0.040$; perifoveal: 107.9 ± 19.0 µm, $P = 0.0007$). Conversely, the inner retina was significantly thinner at the 12-month follow-up visit after initiation of the anti-vascular endothelial growth factor therapy (parafoveal: 90.3 ± 14.8 µm, $P < 0.0001$; perifoveal: 92.0 ± 21.3 µm, $P < 0.0001$). At the 12-month follow-up visit, OCT evidence of alterations of the external limiting membrane and history of previous intraretinal fluid were associated with a greater inner retinal thinning.

Conclusions. The development of exudative neovascularization is associated with significant neuronal loss that may be detected once the exudation is resolved. OCT analysis demonstrated a significant relationship between morphological alterations detected using structural OCT and the amount of inner neuronal loss.

Keywords: retinal ganglion cells, age-related macular degeneration, neovascularization, optical coherence tomography

Age-related macular degeneration (AMD) is a common cause of severe central visual loss among older individuals in the Western world.[1] Intermediate AMD is characterized by the accumulation of large drusen and/or pigmentary alterations, and the late form of AMD is identified by the development of macular neovascularization (MNV) or geographic atrophy.[2,3] Exudation from pathologic type 1 (sub-retinal pigment epithelium), type 2 (subretinal), or type 3 (intraretinal) MNV characterizes the neovascular exudative form of this disease, which affects approximately 10% to 15% of patients with AMD.[2,4,5]

A primary feature of AMD is damage to the unit comprised of the photoreceptors, retinal pigment epithelium (RPE), Bruch's membrane, and choriocapillaris; thus, it is predominantly considered to be an outer retinal disease.[6–11] However, there is increasing evidence suggesting that the inner retina may also be affected from the earliest stages of the disease.[12–14] Importantly, neurodegeneration of the inner retina appears to be associated with disease severity in AMD, with late AMD being characterized by a greater thinning of the inner retinal layers on structural optical coherence tomography (OCT), which may be a surrogate for neuronal loss.[14] Zucchiatti et al.[14] showed that eyes with neovascular AMD are characterized by a significant thinning of the ganglion cell complex (GCC), which is composed of the inner plexiform layer (IPL) and ganglion cell layer (GCL). Similarly, Lee et al.[15] investigated the changes in inner retinal thickness in neovascular AMD subjects undergoing intravitreal therapy with anti-vascular endothelial growth factor (VEGF) injections. Their study demonstrated that a significant progressive thinning of the inner retina may occur in these eyes. Assuming that the survival of ganglion cells is

dependent on VEGF,[16] a progressive decrease in its levels could be associated with neuronal loss and consequent reduction in inner retinal thickness.[15] Alternatively, because photoreceptor damage may result in a chronically reduced input to the inner retina, the inner retinal thinning may be secondary to a disorganized synaptic architecture and transneuronal degeneration over time.[11] Finally, a mechanical compression of the inner retinal neurons from intraretinal and/or subretinal fluids may also lead to the progressive and irreversible death of retinal ganglion cells.[13]

Although the inner neuronal loss occurring in neovascular AMD eyes is well established, no study has investigated the longitudinal modifications to inner retinal layers occurring in intermediate AMD eyes developing MNV. Therefore, the aim of this study was to understand whether the transition from intermediate to neovascular AMD may be associated with longitudinal inner retinal thinning. Also, we lack information concerning the relationships among the morphological characteristics detected with structural OCT B-scans, the clinical features of this disease, and longitudinal inner neuronal loss in patients with neovascular AMD. In the present study, we captured the transition from intermediate to exudative neovascular AMD in order to quantify longitudinal modifications in inner retinal thickness. More importantly, we investigated factors associated with these longitudinal changes, using structural OCT B-scans. Quantitative measurements of the inner retina in the macular region are widely used for the diagnosis, follow-up, and staging of different retinal and optic nerve disorders, including diabetic retinopathy,[17] glaucoma,[18] and ischemic optic neuropathy.[19] Assuming that AMD may frequently coexist with these disorders, it would appear to be of great importance to better characterize changes in the inner retina that occur in intermediate AMD eyes developing exudative MNV. Finally, our results could be helpful to better understand the disease pathophysiology and to identify potential biomarkers for disease progression and new targets for pharmacological treatment.

Methods

The San Raffaele Ethics Committee was notified about this retrospective cohort study, which adhered to the tenets of the Declaration of Helsinki. An informed consent waiver was granted to analyze data that had been previously collected.

Subjects

In this study, consecutive subjects 50 years and older with a diagnosis of intermediate AMD in at least one eye were identified from the San Raffaele Scientific Institute. To be included, subjects were required to develop treatment-naïve exudative neovascular AMD within 3 months after the latest visit with evidence of intermediate AMD. Diagnoses of intermediate and exudative neovascular AMD were determined by clinical examination, structural OCT, and dye angiography, when needed, as previously described.[3,20] After the diagnosis of exudative neovascular AMD, all of the patients received a loading dose of anti-VEGF intravitreal injections followed by either a pro re nata (PRN) or a treat-and-extend regimen at the discretion of the treating physician. Finally, included eyes were required to have evidence of resolved exudation after 12 ± 1 months following initiation of the anti-VEGF therapy in order to avoid exudation confounding the 12-month OCT quantitative and qualitative analyses. Fourteen subjects were excluded because of the presence of signs of exudation at the 12-month follow-up visit.

The following visits were included in the analysis: (1) baseline assessment (0–3 months before evidence of treatment-naïve exudative neovascular AMD); (2) follow-up visit with first evidence of treatment-naïve exudative MNV; (3) 1-month follow-up visit after completion of the loading dose of anti-VEGF therapy; and (4) 12-month follow-up visit after initiation of the anti-VEGF therapy. Exclusion criteria for enrolled eyes were (1) history of vitreoretinal surgery, (2) any maculopathy secondary to causes other than AMD, (3) intraocular pressure higher than 20 mmHg, or (4) diagnosis of diabetic retinopathy or any optic neuropathy, as these disorders may influence changes in the inner retina.[17,19]

At each visit, enrolled subjects had a complete ophthalmologic evaluation, including the measurement of best-corrected visual acuity (BCVA), dilated fundus examination, and multimodal retinal imaging. Visual acuities were tested with Snellen charts and successively transformed to logarithm of the minimal angle of resolution (logMAR) values. Structural OCT was performed with the SPECTRALIS HRA+OCT imaging platform (Heidelberg Engineering, Heidelberg, Germany). Volumetric scans were centered on the fovea and were composed of 19 horizontal B-scans, each of which was comprised of 24 averaged scans, covering an approximately 5.5 × 4.5-mm area centered on the fovea. A minimum signal strength of 25 was required for included scans, as advised by the manufacturer.[21]

OCT Grading

Structural OCT images at baseline and follow-up visits were first reviewed for eligibility by two readers (EB and CB). Successively, the same readers independently graded eligible eyes for qualitative OCT features that may represent signs of MNV exudation, including the presence of intraretinal fluid (IRF), subretinal fluid (SRF), and subretinal hyperreflective material (SHRM), as previously described.[22] This grading was performed at the following visits: (1) follow-up visit with first evidence of treatment-naïve exudative MNV, and (2) 1-month follow-up visit after completion of the loading dose of anti-VEGF therapy. As stated above, the presence of OCT signs of exudation at the 12-month follow-up visit was an exclusion criterion in our analysis; therefore, this assessment was previously performed for eligibility.

OCT images were also graded for qualitative features reflecting distress of the outer retina or RPE. This grading was performed in all scans (i.e., by scrutinizing all B-scans) of the OCT volume within the fovea center subfield (central circle of the Early Treatment Diabetic Retinopathy [ETDRS] grid with a diameter of 1 mm). Final grading was based on the appearance of the layers on all the scrutinized B-scans. The following parameters were assessed:

- *Structural alterations of the outer retina within the foveal region*—The ellipsoid zone (EZ) and external limiting membrane (ELM) bands were assessed for their integrity. These bands were graded as being absent, discontinuous, or intact, as has been done previously.[22,23]

- *Alterations of the RPE within the fovea*—OCT images were also reviewed for the integrity of the RPE. The RPE was also graded as being absent, discontinuous, or intact.[22]

The latter grading was performed at the 12-month follow-up visit after initiation of the anti-VEGF therapy in order to prevent exudation from confounding this analysis. Readers were masked for quantitative values. In those cases in which the two readers were not able to reach a single consensus result, the final decision was made by the senior author (FB).

OCT Quantitative Assessment

At each visit, structural OCT scans of the macula were used to generate and calculate the inner retinal thickness, as previously described.[24] The inner retina represents a combination of the retinal nerve fiber layer (NFL), GCL, and IPL. In brief, the manufacturer's built-in software was used to detect the boundaries of the layers and to measure the thickness of each layer inside the parafoveal and perifoveal ETDRS grid regions (i.e., the inner circle subfield between the inner 1-mm-diameter and middle 3-mm-diameter circles and the outer circle subfield between the middle and outer 6-mm-diameter circles). All B-scans were evaluated by the two readers in order to correct any decentration or segmentation errors before calculating the thickness values.

Statistical Analysis

Statistical calculations were performed using SPSS Statistics 20.0 (IBM, Chicago, IL, USA). To detect departures from a normal distribution, a Shapiro–Wilk test was performed for all variables. Means and standard deviations (SDs) were computed for all quantitative variables. Visual acuities and OCT metrics at baseline and follow-up visits were compared by conducting paired-samples *t*-tests or related-samples Wilcoxon signed-rank test.

Contributory factors affecting average changes in inner retinal thicknesses (dependent variables) were examined using univariable and multivariable linear mixed models. Relationships between average changes in inner retinal thickness (dependent variable) and relevant clinical aspects, including age, gender, diagnosis of diabetes (i.e., established factors associated with a thinning of the inner retina),[25,26] and other morphological parameters, were evaluated using linear regression analysis. Subsequently, multivariable models were constructed that included parameters for which $P < 0.1$ in the univariable analyses. The unweighted *k*-statistic test[27] (intact vs. disrupted/absent for ELM, EZ, and RPE appearances; present vs. absent for IRF, SRF, and SHRM) was used to evaluate agreement between readers in the assessment of OCT qualitative features. Of note, the two readers were able to reach a single consensus result in all cases. False-discovery rate (FDR) correction with Benjamini–Hochberg[28] correction was used to control for testing of multiple novel measures, and a FDR adjusted $P < 0.05$ was determined to be statistically significant.

Results

Characteristics of Patients Included in the Analysis

Eighty eyes from 80 patients with AMD (24 males, 56 females) were enrolled in this study. Mean ± SD age at baseline was 79.9 ± 7.5 years. Table 1 summarizes the demographics and clinical characteristics of this study cohort. The mean ± SD days between the baseline visit and the first visit with evidence of MNV was 69.7 ± 19.3 days. Visual acuity was 0.17 ± 0.17 logMAR at the baseline assessment (i.e., latest visit with evidence of intermediate AMD, from 0–90 days before evidence of treatment-naïve neovascularization), 0.43 ± 0.47 logMAR at the follow-up visit with first evidence of treatment-naïve exudative MNV, 0.35 ± 0.42 logMAR at the 1-month follow-up visit after the loading dose of anti-VEGF therapy, and 0.27 ± 0.23 logMAR at the 12-month follow-up visit following initiation of the anti-VEGF therapy ($P < 0.0001$ in all of the comparisons with baseline values). Out of the 80 eyes, 44 eyes (55.0%) developed a type 1 MNV, and 23 eyes (28.8%) and 13 eyes (16.2%) were affected by type 3 and type 2 MNVs, respectively.

Table 1. Demographic and Clinical Characteristics of Enrolled Patients

Characteristic	
Patients, *n*	80
Eyes, *n*	80
Age (y), mean ± SD	79.9 (7.5)
Gender, *n*	
Male	24
Female	56
Diabetes, *n*	12
Number of anti-VEGF injections in the study period, mean ± SD	5.7 (2.2)

Longitudinal Changes in Inner Retinal Thicknesses

The perifoveal inner retinal thicknesses were 97.6 ± 12.9 µm at baseline, 99.0 ± 12.8 µm at the follow-up visit with first evidence of treatment-naïve exudative MNV ($P = 0.040$), 97.0 ± 13.7 µm at the 1-month follow-up visit after the loading dose of anti-VEGF therapy ($P = 0.521$), and 90.3 ± 14.8 µm at the 12-month follow-up visit after initiation of the anti-VEGF therapy ($P < 0.0001$) (Table 2; Figs. 1, 2). Similarly, the parafoveal inner retinal thicknesses were 103.5 ± 16.2 µm, 107.9 ± 19.0 µm ($P = 0.0007$), 101.8 ± 19.5 µm ($P = 0.154$), and 92.0 ± 21.3 µm ($P < 0.0001$) at baseline and follow-up visits, respectively (Table 2; Figs. 1, 2; Supplementary Figs. S1 and S2). Table 2 and Figure 1 summarize changes in the NFL, GCL, and IPL thicknesses throughout the follow-up.

Regression Analysis at the Follow-Up Visit With First Evidence of Treatment-Naïve Exudative MNV

OCT morphologic characteristics are summarized in Supplementary Figure S3. At the follow-up visit with first evidence of treatment-naïve exudative MNV, 36 eyes (45.0%) showed evidence of IRF, and SRF and SHRM were detected in 57 eyes (71.3%) and 52 eyes (65.0%), respectively. Factors contributing to changes in inner retinal thickness are shown in Table 3. In the multivariable analysis, the presence of IRF was associated with inner retinal thickening in the parafoveal region ($P = 0.011$).

Regression Analysis at the 1-Month Follow-Up Visit After the Loading Dose of Anti-VEGF Therapy

Sixteen eyes (21.2%) showed evidence of IRF, and SRF and SHRM were detected in 24 eyes (30.0%) and 20 eyes

Table 2. Functional and Anatomic Parameters At Different Visits

	Baseline Visit (Latest Evidence of Intermediate AMD)	Follow-Up Visit With First Evidence of Treatment-Naïve Exudative MNV	1-Month Follow-Up Visit After Loading Dose of Anti-VEGF Therapy	12-Month Follow-Up Visit After Initiation of Anti-VEGF Therapy
BCVA (logMAR), mean ± SD	0.17 ± 0.17	0.43 ± 0.47	0.35 ± 0.42	0.27 ± 0.23
P^*	—	<0.0001	<0.0001	<0.0001
Perifoveal NFL thickness (µm), mean ± SD	36.4 ± 5.9	37.1 ± 6.1	35.9 ± 6.3	33.8 ± 6.9
P^*	—	0.048	0.282	<0.0001
Perifoveal GCL thickness (µm), mean ± SD	33.6 ± 5.6	33.5 ± 5.9	32.7 ± 6.0	29.7 ± 6.5
P^*	—	0.634	0.002	<0.0001
Perifoveal IPL thickness (µm), mean ± SD	28.2 ± 3.8	28.9 ± 3.8	28.5 ± 4.4	27.1 ± 3.8
P^*	—	0.002	0.349	0.005
Perifoveal inner retinal thickness (µm), mean ± SD	97.6 ± 12.9	99.0 ± 12.8	97.0 ± 13.7	90.3 ± 14.8
P^*	—	0.040	0.521	<0.0001
Parafoveal NFL thickness (µm), mean ± SD	23.2 ± 4.0	25.9 ± 8.8	23.5 ± 5.3	22.0 ± 4.8
P^*	—	0.002	0.537	0.002
Parafoveal GCL thickness (µm), mean ± SD	44.0 ± 8.5	44.1 ± 8.7	42.0 ± 9.8	37.7 ± 11.2
P^*	—	0.966	0.0003	<0.0001
Parafoveal IPL thickness (µm), mean ± SD	36.5 ± 5.4	38.2 ± 5.6	36.5 ± 6.7	33.5 ± 6.9
P^*	—	0.0005	0.938	<0.0001
Parafoveal inner retinal thickness (µm), mean ± SD	103.5 ± 16.2	107.9 ± 19.0	101.8 ± 19.5	92.0 ± 21.3
P^*	—	0.0007	0.154	<0.0001

* Comparison versus baseline visit.

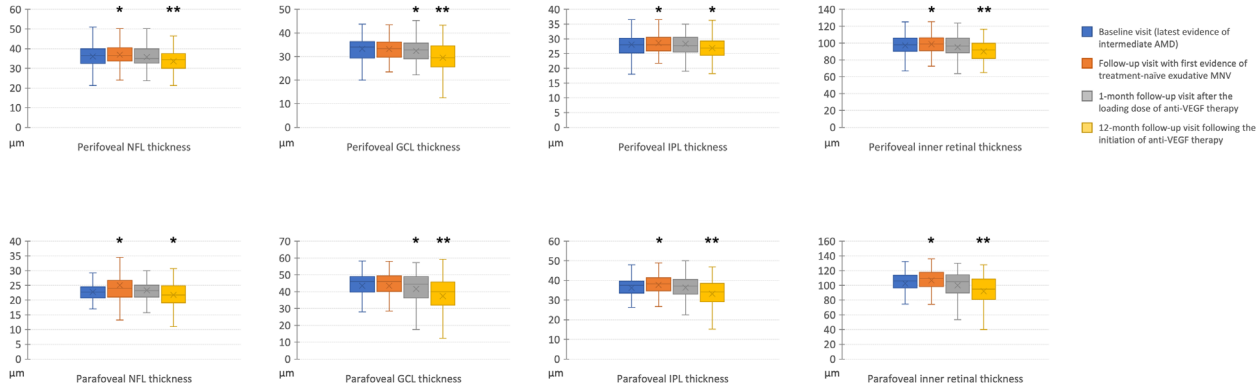

Figure 1. Box-and-whisker plots showing analyzed OCT measurements in patients with AMD. Each *box* indicates mean (*cross within the box*), median (*central horizontal line*), and interquartile range (*horizontal extremes of the box*) values for a specific variable at each visit. The minimum and maximum values correspond to the ends of the whiskers. *Asterisks* highlight significant differences from baseline values (*$P < 0.05$, **$P < 0.0001$). On the *y*-axis, values are reported in micrometers. Values at different visits are organized along the *x*-axis (see the legend in the *upper right corner* for category labels). Details on pairwise comparisons are presented in Table 2.

(25.0%), respectively (Supplementary Fig. S3). In the multivariable analysis, the presence of IRF was associated with inner retinal thickening in the perifoveal ($P = 0.026$) and parafoveal ($P = 0.044$) regions (Table 4). At the 1-month follow-up visit after the loading dose of anti-VEGF therapy, the AMD cohort was further divided into two subgroups according to the presence of OCT signs of exudation. Forty eyes (50.0%) showed signs of exudation (i.e., IRF, SRF, and/or SHRM), and the other 40 eyes (50.0%) did not display OCT signs of exudation. In a subanalysis that included only patients without OCT signs of exudation, perifoveal inner retinal thicknesses were 95.4 ± 13.4 µm at baseline and 93.6 ± 14.2 µm at the 1-month follow-up visit after the loading dose of anti-VEGF therapy ($P = 0.008$). Similarly, parafoveal inner retinal thicknesses were 100.4 ± 18.0 µm and 97.3 ± 21.0 µm at the baseline and 1-month follow-up visits, respectively ($P = 0.022$).

Regression Analysis at the 12-Month Follow-Up Visit After Initiation of the Anti-VEGF Therapy

At the 12-month follow-up visit after initiation of the anti-VEGF therapy, all subjects had an absence of OCT signs of exudation (as per the inclusion criteria). The ELM band was intact in 38 eyes (47.5%); it was graded as disrupted in 27 eyes (33.7%) and absent in 15 eyes (18.8%) (Supplementary Fig. S3). The EZ band was graded as intact, disrupted, or absent in 16 eyes (20.0%), 47 eyes (58.7%), and 17 eyes (21.3%) eyes, respectively (Supplementary Fig. S3). The RPE was intact in 56 eyes (70.0%); it was graded as disrupted in 21 eyes (26.3%) and absent in three eyes (3.7%) (Supplementary Fig. S3). In the multivariable analysis, alterations of the ELM were associated with increased inner retinal thinning in the perifoveal ($P = 0.025$) and parafoveal ($P = 0.027$) regions (Table 5). Furthermore, the OCT evidence of IRF at one of the previous visits was associated with a greater

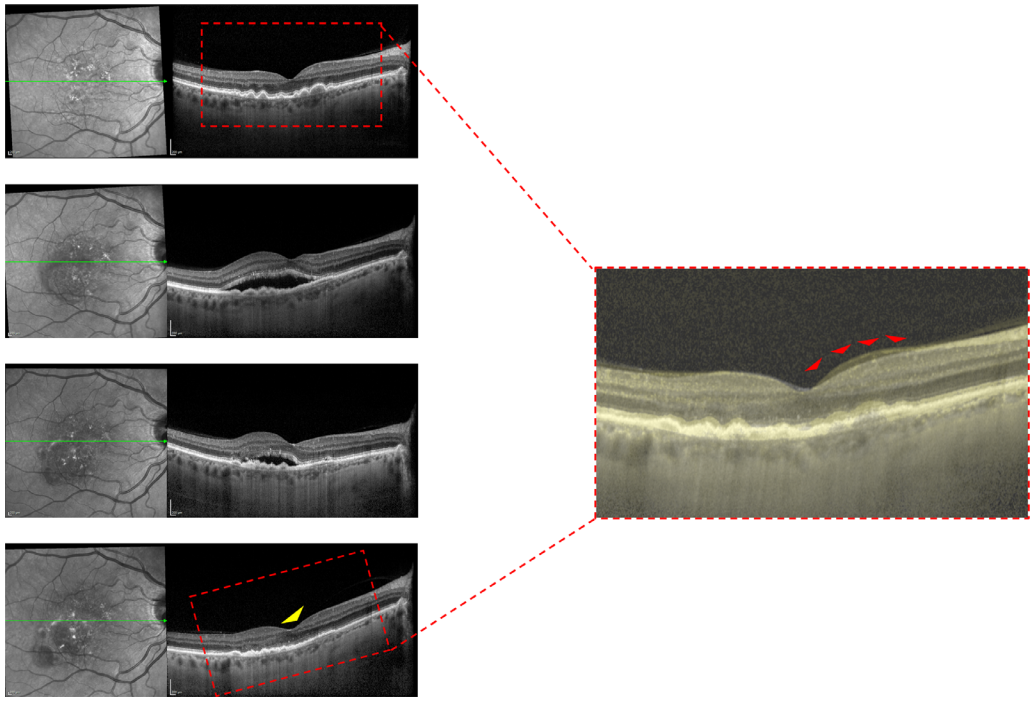

Figure 2. OCT imaging of a patient with AMD developing type 1 MNV and undergoing intravitreal anti-VEGF therapy. (*Left panel*) At baseline (*top row*), the structural OCT B-scan shows the presence of drusenoid pigment epithelial detachments. At the following visit (*second row*), the structural OCT B-scan exhibits a fibrovascular pigment epithelial detachment associated with subretinal fluid. After three intravitreal aflibercept injections (*third row*), structural OCT continues to show subretinal fluid, although it is reduced in amount. At the 12-month follow-up visit (*bottom row*), the structural OCT B-scan shows the resolution of subretinal fluid and absence of signs of exudation. Note the remarkably reduced inner retinal thickness (*yellow arrowhead*). (*Right panel*) Magnified visualizations of the foveal region at baseline (corrected with transparency at 65% and colored *yellow*) and at the 12-month follow-up visit (corrected with transparency at 30%) allow better appreciation of the inner retinal loss (*red arrowheads*) at the last visit.

Table 3. Results of Multivariable Analysis At the Follow-Up Visit With First Evidence of Treatment-Naïve Exudative MNV

	Standardized β Coefficient (95% CI)	*P*	Standardized β Coefficient (SE)	*P*
		Perifovea		
Age	0.143 (−0.066, 0.286)	0.217	—	—
Gender, M/F	−0.169 (−5.174, 0.779)	0.146	—	—
Diabetes, Y/N	1.846 (−3.577, 3.777)	0.957	—	—
MNV type	0.043 (−1.280, 1.877)	0.707	—	—
IRF, Y/N	0.059 (−1.988, 3.349)	0.613	—	—
SRF, Y/N	0.069 (−2.089, 3.886)	0.551	—	—
SHRM, Y/N	−0.123 (−4.231, 1.272)	0.288	—	—
		Parafovea		
Age	−0.061 (−0.396, 0.232)	0.602	−0.047 (−0.422)	0.674
Gender, M/F	0.080 (−3.475, 7.175)	0.491	0.135 (1.196)	0.236
Diabetes, Y/N	−0.100 (−9.322, 3.643)	0.386	−0.157 (−1.402)	0.165
MNV type	0.139 (−1.077, 4.467)	0.277	—	—
IRF, Y/N	0.296 (1.563, 10.613)	0.009[a]	0.290 (2.610)	0.011*
SRF, Y/N	0.068 (−3.717, 6.871)	0.555	—	—
SHRM, Y/N	0.083 (−0.066, 0.286)	0.475	—	—

* Significant *P* values.

inner retinal thinning in the parafoveal region ($P = 0.011$) (Table 5).

Analysis of Fellow Intermediate AMD Eyes

Seventeen out of 80 patients (21.2%) in our study cohort had fellow eyes exhibiting findings consistent with intermediate AMD throughout the follow-up (from baseline to the 12-month follow-up visit). In this group of patients we performed a subanalysis in order to investigate longitudinal changes in the inner retina in eyes not developing MNV. This analysis was performed in order to exclude the notion that inner retinal modifications are secondary to AMD itself, rather than to the development of MNV.

Perifoveal inner retinal thicknesses were 99.1 ± 9.5 µm at baseline and 99.0 ± 8.4 µm at the 12-month follow-up

Table 4. Results of Multivariable Analysis At the 1-Month Follow-Up Visit After the Loading Dose of Anti-VEGF Therapy

	Standardized β Coefficient (95% CI)	*P*	Standardized β Coefficient (SE)	*P*
		Perifovea		
Age	0.163 (−0.059, 0.353)	0.160	0.200 (1.794)	0.077
Gender, M/F	−0.148 (−5.788, 1.236)	0.201	−0.177 (−1.584)	0.117
Diabetes, Y/N	−0.074 (−5.279, 2.942)	0.524	−0.056 (−0.497)	0.621
MNV type	−0.046 (−2.240, 1.492)	0.691	—	—
IRF, Y/N	0.244 (0.318, 7.000)	0.032*	0.255 (2.269)	0.026*
SRF, Y/N	0.065 (−2.786, 4.971)	0.576	—	—
SHRM, Y/N	0.065 (−2.786, 4.971)	0.576	—	—
		Parafovea		
Age	−0.025 (−0.305, 0.246)	0.829	0.006 (0.051)	0.960
Gender, M/F	−0.118 (−7.033, 2.263)	0.310	−0.144 (−1.273)	0.207
Diabetes, Y/N	−0.040 (6.702, 4.717)	0.730	−0.024 (−0.215)	0.830
MNV type	0.142 (−0.910, 3.950)	0.216	—	—
IRF, Y/N	0.303 (1.748, 10.911)	0.007*	0.232 (2.053)	0.044*
SRF, Y/N	0.224 (0.003, 8.829)	0.050*	0.172 (1.524)	0.132
SHRM, Y/N	0.134 (−2.096, 8.029)	0.247	—	—

* Significant *P* values.

Table 5. Results of Multivariable Analysis At the 12-Month Follow-Up Visit After Initiation of Anti-VEGF Therapy

	Standardized β Coefficient (95% CI)	*P*	Standardized β Coefficient (SE)	*P*
		Perifovea		
Age	0.100 (−0.267, 0.672)	0.392	0.109 (0.966)	0.337
Gender, M/F	−0.114 (−11.888, 4.026)	0.328	−0.120 (−1.070)	0.288
Diabetes, Y/N	0.058 (−7.295, 12.216)	0.617	0.096 (0.842)	0.403
MNV type	0.093 (−2.492, 5.869)	0.424	—	—
Number of anti-VEGF injections	−0.182 (−2.807, 0.301)	0.112	—	—
IRF at one of the previous visits, Y/N	−0.088 (−9.801, 4.351)	0.445	—	—
SRF at one of the previous visits, Y/N	−0.118 (−11.986, 3.891)	0.307	—	—
SHRM at one of the previous visits, Y/N	−0.191 (−13.340, 1.126)	0.097	−0.126 (−1.054)	0.295
Appearance of the ELM	−0.252 (−9.660, −0.598)	0.027*	−0.257 (−2.284)	0.025*
Appearance of the EZ	−0.230 (−11.208, −0.146)	0.044*	−0.091 (−0.548)	0.585
Appearance of the RPE	−0.103 (−9.457, 3.581)	0.372	—	—
		Parafovea		
Age	0.008 (−0.402, 0.432)	0.943	−0.005 (−0.046)	0.964
Gender, M/F	−0.129 (−10.975, 3.071)	0.266	−0.185 (−1.656)	0.102
Diabetes, Y/N	0.020 (−7.879, 9.397)	0.862	0.074 (0.656)	0.514
MNV type	−0.061 (−4.695, 2.714)	0.596	—	—
Number of anti-VEGF injections	−0.177 (−2.448, 0.302)	0.124	—	—
IRF at one of the previous visits, Y/N	−0.294 (−14.033, −2.028)	0.009*	−0.288 (−2.592)	0.011*
SRF at one of the previous visits, Y/N	−0.020 (−7.654, 6.416)	0.861	—	—
SHRM at one of the previous visits, Y/N	−0.242 (−13.182, −0.542)	0.034*	−0.151 (−1.215)	0.228
Appearance of the ELM	−0.229 (−9.901, −0.120)	0.045*	−0.252 (−2.276)	0.027*
Appearance of the EZ	−0.216 (−7.926, 0.158)	0.059	−0.140 (−1.169)	0.246
Appearance of the RPE	−0.079 (−7.758, 3.795)	0.496	—	—

* Significant *P* values.

visit ($P = 1.0$). Similarly, parafoveal inner retinal thicknesses were 108.5 ± 13.1 µm and 107.5 ± 11.8 µm ($P = 1.0$) at baseline and follow-up visits, respectively. The perifoveal and parafoveal NFL thicknesses (36.8 ± 5.8 µm and 22.9 ± 1.9 µm at baseline, respectively) did not show significant changes at the 12-month follow-up visit (37.2 ± 5.3 µm and 23.1 ± 1.7 µm; $P = 1.0$ and $P = 1.0$, respectively). The perifoveal and parafoveal GCL thicknesses at baseline (33.6 ± 4.1 µm and 46.8 ± 7.8 µm, respectively) did not change at the 1-year follow-up visit (33.5 ± 3.9 µm and 46.3 ± 7.2 µm; $P = 1.0$ and $P = 1.0$, respectively). The perifoveal and parafoveal IPL thicknesses at baseline (28.8 ± 2.5 µm and 38.8 ± 3.9 µm, respectively) did not show modifications at the 12-month follow-up visit (28.8 ± 2.3 µm and 38.3 ± 3.8 µm; $P = 1.0$ and $P = 1.0$, respectively).

Repeatability

The unweighted *k*-values for interreader repeatability were 0.93 (77/80; 95% confidence interval [CI], 0.85–1.00) for ELM appearance, 0.92 (78/80; 95% CI, 0.81–1.00) for EZ appearance, 1.0 (80/80; 95% CI, 1.00–1.00) for RPE appearance, 0.89 (154/160; 95% CI, 0.82–0.96) for the presence of IRF, 0.95 (156/160; 95% CI, 0.90–1.00) for the presence of IRF, and 0.87 (150/160; 95% CI, 0.79–0.95) for the presence of SHRM.

Discussion

In this longitudinal investigation, we performed a topographical quantitative assessment of the macular neuronal loss in patients with AMD complicated by exudative

MNV and treated with anti-VEGF therapy. Overall, we observed that eyes with AMD are characterized by longitudinal changes in the inner retina. Notably, results of the present study demonstrate a significant relationship between morphological alterations detected using structural OCT and the amount of inner retinal thinning. Among the demographic and clinical factors, age, gender, diagnosis of diabetes, and number of anti-VEGF injections did not significantly impact variations in the inner retina over time after the development of exudative AMD. Because the purpose of our study was to assess the associations between neuronal loss and morphological macular structural features detected using OCT, for which qualitative and quantitative assessments may be impacted by the presence of co-existing conditions or intraretinal/subretinal fluid, our analysis did not include patients not resolving exudation after 1 year of follow-up or patients with evidence of vitreomacular disorders.

As stated above, neovascular AMD eyes are known to be characterized by a thinning of the inner retina.[14,15] However, these previous reports did not account for intersubject factors that might influence the inner retina and confound comparisons across a cohort, assuming that they compared neovascular patients with AMD with either intermediate or healthy subjects. Conversely, in order to overcome the latter limitation, the present longitudinal study captured the transition from intermediate to exudative neovascular stage in a study cohort of patients with AMD.

In our study, the inner retinal thickness was demonstrated to be significantly increased at the follow-up visit with first evidence of treatment-naïve neovascular AMD. The inner retinal thickening appeared to be mainly related to intraretinal exudation, as revealed by multivariable analysis. Conversely, we observed a significant decrease in inner retinal thickness after 1 year of follow-up after the development of exudative MNV. We also performed a single-layer analysis showing that each retinal layer constituting the inner retina (i.e., NFL, GCL, and IPL) was significantly thinner at this follow-up compared with the latest visit with evidence of intermediate AMD. In contrast, no significant changes in inner retinal thickness were detected at the 1-month follow-up visit after conclusion of the loading dose of anti-VEGF therapy. Of note, we further divided our AMD cohort into two subgroups according to the presence of OCT signs of exudation at the latter follow-up visit. Interestingly, in this additional analysis, the decrease in inner retinal thickness reached statistical significance in eyes without signs of exudation.

Taken together, our results suggest that the presence of intraretinal exudation during the development of AMD-associated MNV can cause an early thickening of the inner retina. When intraretinal exudation that has been detected by structural OCT is resolved, significant inner neuronal loss may be detected. We additionally included fellow eyes with intermediate AMD (and unilateral MNV throughout the study period) in our comparative analysis and demonstrated that the fellow intermediate AMD eyes displayed no significant changes in the inner retina. This finding also indirectly supports the concept that the development of MNV may be causative of inner neuronal loss.

Notably, the present study highlights the distinctive relationship between morphological features detected using structural OCT and progressive inner retinal thinning in neovascular AMD eyes. There are at least three potential hypotheses that may explain the neuronal loss occurring after the transition from intermediate to exudative neovascular AMD: (1) postreceptor functional loss, (2) mechanical tension,[13] and (3) reduced amounts of VEGF, which is an important mediator of trophic support for ganglion cells.[15] According to the first hypothesis, the neuronal loss may be secondary to disorganized synaptic architecture and progressive transneuronal degeneration, due to the decreased input to the inner retina subsequent to the photoreceptor harm.[29,30] Sullivan et al.[30] performed a histopathological study on the postmortem retinas from subjects affected by AMD. Their study showed that degeneration of photoreceptors is followed by either death or migration out of the retina of the inner retinal neurons. Using structural OCT, the postreceptor functional loss hypothesis was investigated in eyes affected by intermediate AMD.[11] That study demonstrated a significant relationship between inner neuronal loss and photoreceptor damage in these eyes, suggesting that a pathological dysregulation between these two neuroretinal structures (i.e., photoreceptor and inner retina) becomes apparent at the earliest stages of the disease.

In this study, the presence of specific qualitative changes in the outer retina on structural OCT images was associated with worse inner retinal thinning after the transition from intermediate to neovascular AMD. We considered the average change in inner retinal thickness between baseline and 12-month follow-up visits to be a dependent variable, and we identified a direct relationship with elements defining damage of the outer retina (i.e., ELM appearance), even after accounting for confounding factors, including age and presence of diabetes, which are known to modify inner retinal thickness. Several studies that have adopted structural OCT have observed that eyes with resolved exudation secondary to neovascular AMD may feature an attenuation of the outer retinal layers.[22,23] Assuming that AMD is considered to be primarily an outer retina disease and given that inner neuronal loss cannot induce a secondary impairment of the photoreceptors, our results would appear to support the postreceptoral hypothesis regarding the inner retinal thinning observed after the transition from intermediate to exudative neovascular AMD.

Given that reflection signal located at the level of the EZ is thought to colocalize with photoreceptor inner segment ellipsoids that incorporate densely packed mitochondria,[11,31,32] decreased visualization of the EZ may reflect either a functional or a structural photoreceptor injury. In contrast, the signal arising from the ELM appears to correspond to intercellular junctions between photoreceptor and Müller cells, and it is thus considered to be a better surrogate for photoreceptor structure.[33] In addition, the structural OCT analysis in our study cohort revealed that the frequency of the appearance of disrupted or absent ELMs was significantly lower than for the EZ. Finally, previous studies have highlighted the functional importance of the ELM in neovascular AMD eyes and indicate that the status of the ELM may be considered to be a better predictor of visual acuity in these eyes.[22,23] Therefore, taking these findings together, it seems reasonable that disrupted or absent appearance of the ELM may reflect worse photoreceptor damage in neovascular AMD eyes. This latter aspect might partially account for the lack of a significant relationship between EZ status and average change in inner retinal thickness between baseline and the 12-month follow-up visits. Conversely, our study further emphasizes the functional importance of the

Investigative Ophthalmology & Visual Science

ELM in neovascular AMD, assuming a distinctive relationship between ELM status and neuronal loss displayed in eyes converting from intermediate to exudative neovascular AMD.

Another possible hypothesis for the inner retinal thinning occurring in AMD eyes transitioning from intermediate to neovascular status is mechanical tension to the inner retinal layers caused by exudation leading to secondary retinal ganglion cell damage.[13] Our results, would seem to support this hypothesis. Indeed, when the presence of intraretinal fluid was a covariate in our multiple regression analyses, we observed that this variable was a strong predictor of average change in inner retinal thickness between baseline and 12-month follow-up visits. The presence of intraretinal fluid may disrupt pathways transmitting visual information from photoreceptors to retinal ganglion cells and may eventually result in neuronal loss.

Our study does have limitations, including its retrospective nature, which may be susceptible to selection and ascertainment bias; however, a prospective study would be difficult to design, as it is not possible to predict the timing of neovascular AMD development. Furthermore, our study cohort consisted of subjects with resolved exudation at the 12-month follow-up visit after initiation of the anti-VEGF therapy; therefore, our results may vary in other cases. Conversely, the presence of OCT signs of exudation may result in an erroneous qualitative or quantitative analysis.[34] Thus, we felt the safer strategy was to just exclude cases with OCT evidence of exudation at the last follow-up visit. A final limitation is intrinsic to OCT technology, as variations in transverse magnification primarily caused by differences in axial length may have an impact on individual retinal thickness measurements.[35] However, individual differences in retinal image magnification may be marginal in our analysis, which assessed longitudinal changes in retinal layer measurements rather than differences in these metrics between two groups.

In conclusion, this study investigated longitudinal changes in the inner retina occurring after the transition from intermediate to exudative neovascular AMD. We observed that the development of exudative neovascularization was associated with significant neuronal loss that can be detected when the exudation is resolved. Notably, we demonstrated a significant relationship between morphological alterations detected using structural OCT (i.e., ELM status and presence of IRF) and the amount of inner retinal thinning. Our findings may help broaden our understanding regarding the pathogenesis and natural history of AMD. Importantly, these results must be taken into account in clinical practice, as quantitative measurements of the inner retina in the macular region are widely used for the diagnosis, follow-up, and staging of different retinal and optic nerve disorders. Finally, our findings may guide the development of optimal anatomic targets in neovascular exudative AMD subjects undergoing anti-VEGF therapy.

Acknowledgments

Disclosure: **E. Borrelli**, None; **C. Barresi**, None; **G. Lari**, None; **A. Berni**, None; **M. Battista**, None; **M. Reibaldi**, None; **M.L. Cascavilla**, None; **F. Bandello**, Alcon (C), Alimera Sciences (C), Allergan (C), Farmila Théa (C), Bayer Schering Pharma (C), Bausch + Lomb (C), Genentech (C), Hoffmann-La Roche (C), Novagali Pharma (C), Novartis (C), Sanofi-Aventis (C), ThromboGenics (C), Zeiss (C)

References

1. Friedman DS, O'Colmain BJ, Muñoz B, et al. Prevalence of age-related macular degeneration in the United States. *Arch Ophthalmol*. 2004;122(4):564–572.
2. Spaide RF, Jaffe GJ, Sarraf D, et al. Consensus nomenclature for reporting neovascular age-related macular degeneration data: Consensus on Neovascular Age-Related Macular Degeneration Nomenclature Study Group. *Ophthalmology*. 2020;127(5):616–636.
3. Ferris FLIII,Wilkinson CP, Bird A, et al. Clinical classification of age-related macular degeneration. *Ophthalmology*. 2013;120(4):844–851.
4. Ferris FLIII,Fine SL, Hyman L. Age-related macular degeneration and blindness due to neovascular maculopathy. *Arch Ophthalmol*. 1984;102(11):1640–1642.
5. Colijn JM, Buitendijk GHS, Prokofyeva E, et al. Prevalence of age-related macular degeneration in Europe: The past and the future. *Ophthalmology*. 2017;124(12):1753–1763.
6. Borrelli E, Uji A, Sarraf D, Sadda SR. Alterations in the choriocapillaris in intermediate age-related macular degeneration. *Invest Ophthalmol Vis Sci*. 2017;58(11):4792–4798.
7. Borrelli E, Shi Y, Uji A, et al. Topographical analysis of the choriocapillaris in intermediate age-related macular degeneration. *Am J Ophthalmol*. 2018;196:34–43.
8. Nassisi M, Shi Y, Fan W, et al. Choriocapillaris impairment around the atrophic lesions in patients with geographic atrophy: A swept-source optical coherence tomography angiography study. *Br J Ophthalmol*. 2019;103(7):911–917.
9. Borrelli E, Mastropasqua R, Senatore A, et al. Impact of choriocapillaris flow on multifocal electroretinography in intermediate age-related macular degeneration eyes. *Invest Ophthalmol Vis Sci*. 2018;59(4):AMD25.
10. Borrelli E, Souied EH, Freund KBB, et al. Reduced choriocapillaris flow in eyes with type 3 neovascularization due to age-related macular degeneration. *Retina*. 2018;38(10):1968–1976.
11. Borrelli E, Abdelfattah N, Uji A, Nittala M, Boyer DS, Sadda SR. Postreceptor neuronal loss in intermediate age-related macular degeneration. *Am J Ophthalmol*. 2017;181:1–11.
12. Savastano MC, Minnella AM, Tamburrino A, Giovinco G, Ventre S, Falsini B. Differential vulnerability of retinal layers to early age-related macular degeneration: Evidence by SD-OCT segmentation analysis. *Invest Ophthalmol Vis Sci*. 2014;55(1):560–566.
13. Lee EK, Yu HG. Ganglion cell-inner plexiform layer and peripapillary retinal nerve fiber layer thicknesses in age-related macular degeneration. *Invest Ophthalmol Vis Sci*. 2015;56(6):3976–3983.
14. Zucchiatti I, Parodi MB, Pierro L, et al. Macular ganglion cell complex and retinal nerve fiber layer comparison in different stages of age-related macular degeneration. *Am J Ophthalmol*. 2015;160(3):602–607.e1.
15. Lee SW, Sim HE, Park JY, et al. Changes in inner retinal layer thickness in patients with exudative age-related macular degeneration during treatment with anti-vascular endothelial growth factor. *Medicine (Baltimore)*. 2020;99(17):e19955.
16. Nishijima K, Ng YS, Zhong L, et al. Vascular endothelial growth factor-A is a survival factor for retinal neurons and a critical neuroprotectant during the adaptive response to ischemic injury. *Am J Pathol*. 2007;171(1):53–67.
17. Borrelli E, Grosso D, Barresi C, et al. Long-term visual outcomes and morphologic biomarkers of vision loss in eyes with diabetic macular edema treated with anti-VEGF therapy. *Am J Ophthalmol*. 2022;235:80–89.

18. Tan O, Chopra V, Lu AT-H, et al. Detection of macular ganglion cell loss in glaucoma by Fourier-domain optical coherence tomography. *Ophthalmology*. 2009;116(12):2302–2305.
19. Aggarwal D, Tan O, Huang D, Sadun AA. Patterns of ganglion cell complex and nerve fiber layer loss in nonarteritic ischemic optic neuropathy by Fourier-domain optical coherence tomography. *Invest Ophthalmol Vis Sci*. 2012;53(8):4539–4545.
20. Borrelli E, Bandello F, Souied EH, et al. Neovascular age-related macular degeneration: Advancement in retinal imaging builds a bridge between histopathology and clinical findings. *Graefes Arch Clin Exp Ophthalmol*. 2022;260(7):2087–2093.
21. Huang Y, Gangaputra S, Lee KE, et al. Signal quality assessment of retinal optical coherence tomography images. *Invest Ophthalmol Vis Sci*. 2012;53(4):2133–2141.
22. Fang M, Chanwimol K, Maram J, et al. Morphological characteristics of eyes with neovascular age-related macular degeneration and good long-term visual outcomes after anti-VEGF therapy. *Br J Ophthalmol*. 2023;107(3):399–405.
23. Oishi A, Hata M, Shimozono M, Mandai M, Nishida A, Kurimoto Y. The significance of external limiting membrane status for visual acuity in age-related macular degeneration. *Am J Ophthalmol*. 2010;150(1):27–32.e1.
24. Li ST, Wang XN, Du XH, Wu Q. Comparison of spectral-domain optical coherence tomography for intraretinal layers thickness measurements between healthy and diabetic eyes among Chinese adults. *PLoS One*. 2017;12(5):e0177515.
25. Kashani AH, Zimmer-Galler IE, Shah SM, et al. Retinal thickness analysis by race, gender, and age using Stratus OCT. *Am J Ophthalmol*. 2010;149(3):496–502.e1.
26. Pinilla I, Idoipe M, Perdices L, et al. Changes in total and inner retinal thicknesses in type 1 diabetes with no retinopathy after 8 years of follow-up. *Retina*. 2020;40(7):1379–1386.
27. Landis JR, Koch GG. The measurement of observer agreement for categorical data. *Biometrics*. 1977;33(1):159–174.
28. Benjamini Y, Hochberg Y. Controlling the false discovery rate: A practical and powerful approach to multiple testing. *J R Stat Soc Ser B*. 1995;57(1):289–300.
29. Hendrickson A, Warner CE, Possin D, Huang J, Kwan WC, Bourne JA. Retrograde transneuronal degeneration in the retina and lateral geniculate nucleus of the V1-lesioned marmoset monkey. *Brain Struct Funct*. 2015;220(1):351–360.
30. Sullivan R, Penfold P, Pow DV. Neuronal migration and glial remodeling in degenerating retinas of aged rats and in nonneovascular AMD. *Invest Ophthalmol Vis Sci*. 2003;44(2):856–865.
31. Staurenghi G, Sadda S, Chakravarthy U, Spaide RF, International Nomenclature for Optical Coherence Tomography (IN•OCT) Panel. Proposed lexicon for anatomic landmarks in normal posterior segment spectral-domain optical coherence tomography: The IN•OCT consensus. *Ophthalmology*. 2014;121(8):1572–1578.
32. Borrelli E, Palmieri M, Viggiano P, Ferro G, Mastropasqua R. Photoreceptor damage in diabetic choroidopathy. *Retina*. 2020;40(6):1062–1069.
33. Williams DS, Arikawa K, Paallysaho T. Cytoskeletal components of the adherens junctions between the photoreceptors and the supportive Müller cells. *J Comp Neurol*. 1990;295(1):155–164.
34. Hwang YH, Kim MK, Kim DW. Segmentation errors in macular ganglion cell analysis as determined by optical coherence tomography. *Ophthalmology*. 2016;123(5):950–958.
35. Niyazmand H, Lingham G, Sanfilippo PG, et al. The effect of transverse ocular magnification adjustment on macular thickness profile in different refractive errors in community-based adults. *PLoS One*. 2022;17(4):e0266909.

Investigative Ophthalmology & Visual Science